MAGNETIC MEDIA, IMAGING

Magnetic imaging is used to examine small-scale magnetic features within materials, often on the submicrometer scale. There are several techniques available that give complementary information about the magnetization within and at the surface of a material and the magnetic field outside the material. These techniques can be used for a range of magnetic materials, but this article emphasizes applications to magnetic storage media. Although many of the examples cited refer to hard disk media, the techniques are equally applicable to flexible or magnetooptical media. Magnetic imaging provides insight into the magnetic structure of patterns of data written onto media and the mechanisms for magnetization reversal in media.

We will discuss the capabilities, limitations, and resolution of various magnetic imaging techniques based on different physical principles. Lorentz transmission electron microscopy (LTEM) and electron holography (EH) are transmission electron microscope techniques sensitive to the magnetic field experienced by a beam of electrons passing through a sample. Scanning electron microscopy with polarization analysis (SEMPA) and the magnetooptical Kerr effect (MOKE) are sensitive to the magnetization state of the material near the surface of a sample. Bitter patterns, magnetic force microscopy (MFM), and EH are used to determine the magnetic field outside the medium. For each technique, we give a brief description of the principle on which it is based, discuss the information that it provides, and describe its advantages and limitations. We compare these methods and assess future developments in magnetic imaging.

BITTER PATTERNS

Early domain images were obtained using the Bitter method (1,2). Bitter patterns are formed by applying a colloidal suspension of fine ferromagnetic particles to the surface of the ferromagnetic material of interest. The particle pattern delineates the magnetic field lines at the surface and is observed in an optical microscope. The suspension, traditionally a precipitate of fine Fe_3O_4 particles with a dispersant, can be placed directly on the magnetic surface or applied using an applicator pen. Both the optical microscope and the particle size limit submicron analysis. Thus, low-frequency bit patterns on a hard disk can be observed for location purposes, but micromagnetic details cannot be analyzed. To achieve higher-resolution imaging, submicron ferromagnetic particles can be dispersed on the surface and observed by scanning or transmission electron microscopy. This allows magnification of up to 20,000× and resolution below 0.1 μm, but further advances remain limited by formation, dispersion, and alignment of the ultrafine magnetic particles (3). However, 80 nm resolution has recently been reported using the Bitter technique (4) by forming 20 nm magnetic particles by sputtering and depositing them onto written media in a vacuum chamber and, then observing the sample by scanning electron microscopy.

MAGNETOOPTICAL KERR EFFECT

The magnetooptical Kerr effect is commonly used to study magnetic structure (5–10). In this technique, plane-polarized light is reflected from the surface of a magnetic material. The plane of polarization is rotated by the Kerr angle, typically of order 1°, on reflection from the surface, with the sense of the rotation dependent on the direction of magnetization. By passing the reflected beam though a polarizer, magnetic contrast is observed such that domains or domain walls show as different gray levels. This is performed using an optical microscope with magnification of up to about 1000×. By varying the geometry of the optical system, the contrast can be made sensitive to domain walls or to the magnetization of the magnetic domains themselves, and measurements may also be performed in transmission mode for transparent materials. In transmission mode, the rotation of the plane of polarization of light is known as the Faraday effect. MOKE, like the optical Bitter method, is limited by the wavelength of light, but has been particularly useful for imaging domain patterns in samples such as permalloy pole pieces in recording heads. Advantages of the MOKE technique include the ability to do high-frequency dynamic imaging and to image through thick transparent materials in a nondestructive way without need for special sample preparation.

Near field optical microscopy (NFOM) or scanning near-field optical microscopy (SNOM) combined with Kerr magnetometry has recently been shown to offer dramatic improvement over standard MOKE resolution (7–10). Figure 1 shows a NFOM image of bits written onto a Co/Pt multilayer film (8). The best-case resolution in NFOM is below 50 nm, which is approaching the useful range for imaging details of recording media having bit sizes that are currently on the order of 200 nm × 2000 nm. Resolution improvement beyond this may be difficult owing to the combination of rapid resolution loss with increasing probe– or lens–media spacing, finite lens size, and media surface roughness. Continuing improvement of the NFOM technique may be anticipated as it is developed for other applications such as optical data storage technology. MOKE will continue to be used for analysis of larger-scale domain patterns in recording heads and in particular for dynamic measurements.

LORENTZ TRANSMISSION ELECTRON MICROSCOPY

Lorentz transmission electron microscopy (11–14) is based on a transmission electron microscope (TEM), in which an electron source emits electrons, which are accelerated by an accurate electric field and focused by a series of condenser lenses, generating suitable illumination at a specimen. The electron beam is transmitted through the thin specimen and focused by the objective lens to produce both a diffraction pattern at the back focal plane of the lens and an image at the image plane of the lens. By use of appropriate apertures and imaging conditions, a variety of data can be obtained including bright-field, dark-field, and high-resolution images and diffraction patterns. In LTEM, the imaging conditions are se-

J. Webster (ed.), *Wiley Encyclopedia of Electrical and Electronics Engineering*. Copyright © 1999 John Wiley & Sons, Inc.

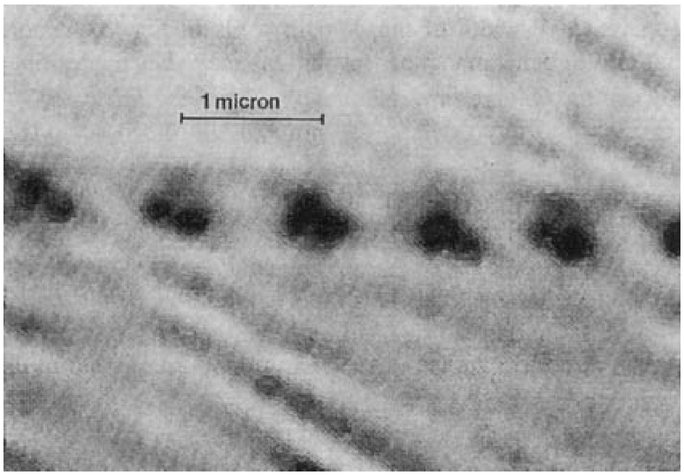

Figure 1. Magnetooptical Kerr effect near-field optical microscopy image of five individual 0.5 μm diameter magnetic domains in a Co/Pt multilayer film with out-of-plane magnetization (8). Reprinted with permission of the authors and the American Institute of Physics.

lected to display magnetic contrast in the specimen. This is based on deflection of the electrons by the Lorentz force. The Lorentz force is given by the vector product $-e(\boldsymbol{v} \times \boldsymbol{B})$, where e is the electron charge, $\boldsymbol{v}$ the electron velocity, and $\boldsymbol{B}$ the magnetic flux density. This deflects the electrons in a direction perpendicular to both $\boldsymbol{B}$ and $\boldsymbol{v}$. The total deflection angle is proportional to the in-plane component (i.e., the component perpendicular to the electron trajectory) of $\boldsymbol{B}$ integrated along the electron trajectory. If we neglect the effect of the field outside the specimen and assume that the magnetization is constant through the thickness of the specimen then the angular deflection is proportional to the in-plane component of the magnetization and to the sample thickness.

The deflection angle of the electrons can be detected in several ways.

1. *Low-angle diffraction mode.* The angular deflection of electrons results in a shift of the electron beam and can be measured directly from the displacement of the transmission spot (the center spot in the diffraction pattern) at the back focal plane of the imaging lens.
2. *Foucault mode.* The image is observed with an aperture placed in the diffraction pattern at the back focal plane. This aperture is off-centered, allowing the passage only of beams deflected in a certain direction. Domains with magnetizations that deflect electrons in that direction will appear bright while others appear dark. By manipulating the aperture position, one can identify the in-plane component of the magnetization in different domains of the specimen.
3. *Fresnel mode.* The image is observed in an out-of-focus condition. The Lorentz force effectively deflects the electrons as they are transmitted through a magnetic domain. This deflection is not visible in the in-focus image, but as the image is defocused, the domain image is shifted normal to its magnetization direction, which causes different domain images to overlap or move apart, giving rise to magnetic contrast wherever the magnetization component parallel to a domain boundary changes magnitude and/or direction across the boundary.
4. *Differential phase contrast mode.* This method is implemented in a scanning transmission electron microscope, in which incident electrons are focused to a fine probe and scanned across the specimen. The angular deflection of the beam is measured using a quadrant detector. These signals quantitatively measure the in-plane magnetization component in the small analyzed area. By scanning the probe across the specimen, a map of the in-plane magnetization component can be determined.

Foucault and Fresnel modes are simple to implement and are generally used for qualitative measurement. The former detects magnetization inside domains while the latter is sensitive to variation of magnetization due to, for example, domain walls. The differential phase contrast mode can provide quantitative information about the magnetization distribution in the specimen. The wave nature of electrons also allows the use of interference methods to detect magnetic information. Such methods produce interferograms between a reference beam and a sample-modulated beam, from which both the phase and amplitude of the electron wave exiting the specimen can be extracted. The major interference method is electron holography, which is discussed separately in this article. Coherent Foucault imaging, in which the opaque aperture used in the Foucault mode is replaced with a phase-shifting aperture, is also possible.

In a conventional TEM the specimen is placed as close as possible to the objective lens to achieve high resolution (about 0.2 nm or better resolution) and high magnification. However, the magnetic field from the lens distorts or erases the magnetization pattern in a magnetic sample, so during LTEM the objective lens is turned off and the intermediate lens serves as the imaging lens. Ideally, an additional lens is installed farther from the specimen. The lens resolution is, however, reduced to about 2 nm to 3 nm. A field emission electron source is also desirable to obtain optimum magnetic contrast. Sample preparation consists of cutting a 3 mm diameter sample and thinning it until it is transparent to electrons. Since the angular deflection of the electrons is proportional to both the magnetization and the magnetic film thickness, the ideal LTEM specimen will have uniform thickness but needs to be thin enough ($<$50 nm to 100 nm) to be transparent to electrons. Most TEM specimen preparation methods produce wedge-shaped specimens, but a combined mechanical thinning and chemical etching technique has been developed for Co-alloy/Cr hard-disk media that produces a large area of uniform film suitable for LTEM (15).

Many applications of these methods have been demonstrated. For instance, magnetization reversal processes in TbCo-biased spin valves (16) and magnetization vortices in CoCrTa hard-disk media (15) have been imaged by the Fresnel mode. Domain walls and magnetization processes in NiFe have been imaged at high resolution by the Foucault mode (17,18). Stray magnetic fields outside write heads have been imaged by both differential phase contrast (DPC) and Foucault modes (19). Tomographic reconstruction of the three-dimensional magnetic field was performed by analyzing a set of DPC images taken in different directions. However, the need for sophisticated TEM facilities has limited the use of LTEM

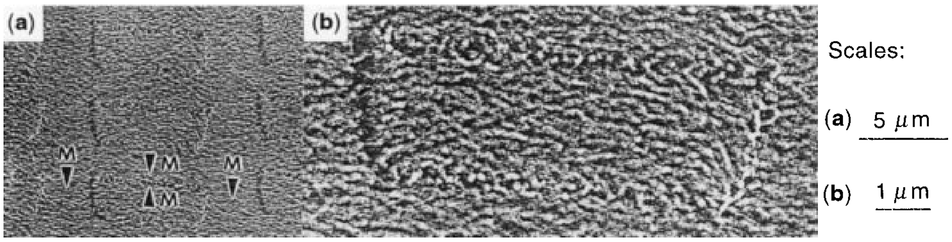

Figure 2. Fresnel LTEM image of low-density data tracks written in an initially dc-erased CoCrTa/Cr longitudinal hard disk. Parts (a) and (b) represent different magnifications. Arrows show the magnetization direction. Tracks run from top to bottom of the figure (15). Reprinted with permission of the authors and the Institute of Electrical and Electronic Engineers.

to relatively few laboratories. Figure 2 shows a Fresnel mode image of magnetic bits written in a magnetic hard disk (15). Boundaries between the magnetic bits can clearly be seen. Within the bits and in the intertrack regions, ripple patterns indicate local fluctuations in magnetization direction. Details on a scale of 50 nm to 100 nm may be resolved.

SCANNING ELECTRON MICROSCOPE–BASED TECHNIQUES

Magnetic imaging due to the Lorentz force can also be carried out using a scanning electron microscope (SEM). In a conventional SEM, the sample is scanned by a beam of electrons of energy between about 1 kV and 20 kV. The yield of secondary (low-energy) electrons emitted from the surface gives an image of surface topography, while the yield of primary (high-energy backscattered) electrons is sensitive to atomic number and hence composition. Deflection of electrons by magnetic fields in or near the sample additionally provides information on the magnetization distribution in the sample (20). In type I imaging, deflection of secondary electrons by the magnetic field above the sample surface is observed using an asymmetric detector. This has been applied to detect, for instance, stray fields outside magnetic recording heads (21). In type II imaging, the deflection of obliquely incident electrons by internal magnetic fields can be observed. The electrons are deflected towards or away from the surface depending on the direction of magnetization, and this alters the yield of secondary electrons. The different electron yield from domains of different magnetization leads to contrast between domains. Contrast arising from domain walls can also be obtained from electrons incident normally or obliquely. These methods can be used to probe the depth dependence of magnetic structure (22). Imaging is done under ultrahigh-vacuum conditions with sample preparation limited to removal of surface layers or contaminants.

Spin-polarized SEM (SEMPA) is a SEM-based technique that can provide information on the three-dimensional magnetization vector of the sample (23–29). It is based on the observation that secondary electrons emitted from a ferromagnet retain their original spin orientation as they leave the sample. A vector map of magnetization can be measured by analyzing the three components of polarization using a finely focused electron beam. SEMPA is surface sensitive due to the small escape depth of secondary electrons of a few nanometers. SEMPA can probe the surface magnetization vector with a best-case resolution of about 20 nm, but poor efficiency makes for slow data aquisition and scans take 30 min to a few hours. Resolution is affected only slightly by surface topography or fringing fields outside the sample.

The SEMPA instrument consists of an electron source and optical column with 10 keV to 50 keV accelerating voltage, a secondary-electron collector, and a set of three orthogonal spin detectors made from gold targets. Spin detectors have been designed to measure both high-energy electrons (20 keV to 100 keV), which are insensitive to the cleanliness of the gold target surface, or low-energy electrons (around 100 eV), for which the detectors are less bulky but require extremely clean gold surfaces. Figure 3 shows a SEMPA image of a magnetic hard disk written with bits at a density of 100 and 240 kfci (kiloflux changes per inch) (39×10^3 and 94×10^3 flux changes cm^{-1}) (28). This image shows the component of magnetization parallel to the data track. A further development of SEMPA is represented by spin-polarized low-energy electron microscopy (SPLEEM). The physics and resolution of SPLEEM are similar to SEMPA (30,31) but SPLEEM offers parallel detection, hence higher data rates, athough there is greater environment sensitivity owing to the use of electrons with energies below 10 eV.

ELECTRON HOLOGRAPHY

Electron holography (EH) is a method based on TEM, in which both the amplitude and the phase of the electron beam are recorded as it passes through a sample. Conventional TEM records only the amplitude of the transmitted beam. By detecting phase shifts of the transmitted beam caused by electric or magnetic fields within the sample, high-resolution images of the electric or magnetic field distribution may be made. Electron holography was proposed in the 1940s (32,33)

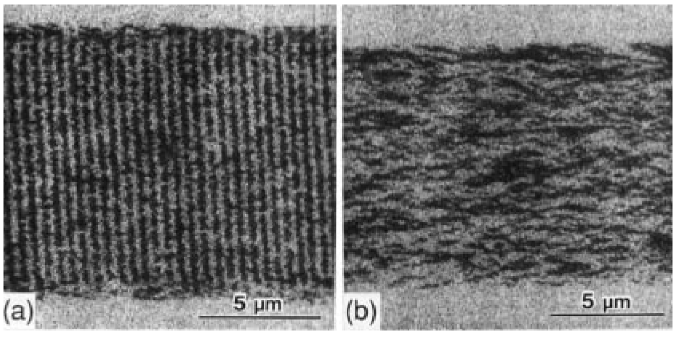

Figure 3. SEMPA image of data tracks written in a hard disk at (a) 100 kfci and (b) 240 kfci after removal of the carbon overcoat. The tracks run left to right. The component of magnetization parallel to the track is shown. In (b), significant percolation is visible and bits cannot be resolved (28). Reprinted with permission of the authors and Oxford University Press.

but has become more widely used as high-intensity field-emission electron sources have been developed. A range of holographic techniques and applications has been described (34–36).

EH can be used for quantitative measurements of magnetic field distribution within or near a sample at high resolution. The technique uses a TEM with an electrostatic biprism (37), which splits the incident electron beam. Part of the beam passes through the sample while a reference beam passes through a hole in the sample (the absolute mode) or through an adjacent region of the sample (the differential mode) (38). The beams are recombined to form a hologram consisting of interference fringes. Phase changes to the electron beam passing through the specimen are detected as shifts in the fringes. For a sample of uniform thickness and composition, shifts in the fringes correlate directly with the magnetic field within the plane of the sample averaged through the sample thickness, so, for example, magnetic domain walls can be imaged as shifts in the fringes. The hologram needs to be reconstructed optically or by computer simulation to yield the phase differences that contributed to it. By measuring phase changes caused by a reference sample, for instance, a nickel film of known thickness, the system can be calibrated so that the magnetic field within the sample can be measured quantitatively.

This method has been used to image magnetization within films, for instance, to show Néel walls within a Ni sample and magnetization in the Co layers of a Co/Pd multilayer (38). It can also be used to image magnetic fields outside samples such as magnetic force microscopy tips (39) and magnetic heads (40). The spatial resolution of EH can be of the order of 1 nm (34). Although this technique requires specialized equipment and analysis, it is valuable in providing quantitative data for comparison with other techniques such as Lorentz microscopy and MFM.

MAGNETIC FORCE MICROSCOPY

Magnetic force microscopy (MFM) has become the most important tool for imaging magnetization patterns in a large number of technologically and scientifically important applications. This includes imaging of magnetic recording media (41), recording heads (42), biomagnetic structures (43), and numerous other materials (44). In many cases, postprocessing of MFM data provides insights into the micromagnetic details of magnetization processes, for instance, quantification of track-edge percolation phenomena in magnetic thin film media (45). Significantly, MFM can be used to study magnetization reversal in individual particles by imaging in a varying externally applied field (46). Examples of MFM images of recorded data tracks are given in Fig. 4 (45).

MFM was developed as an extension of atomic force microscopy (AFM) (47). MFM relies largely on the same instrumentation techniques as AFM but uses a magnetic tip to sense stray magnetic fields above the sample surface. The essential elements of the instrument are a magnetic tip, which is mounted on a cantilever, piezoelectric motors for raster scanning and for control of vertical tip motion, and laser optics for detection of vertical tip response (48). Tips are commonly silicon pyramids coated with a CoCr film (49). Other tip geometries have been developed to improve resolution (50,51). Furthermore, in order to image soft magnetic materials, tips have also been coated with soft or superparamagnetic materials (52). Imaging is performed in ambient atmosphere with minimal sample preparation.

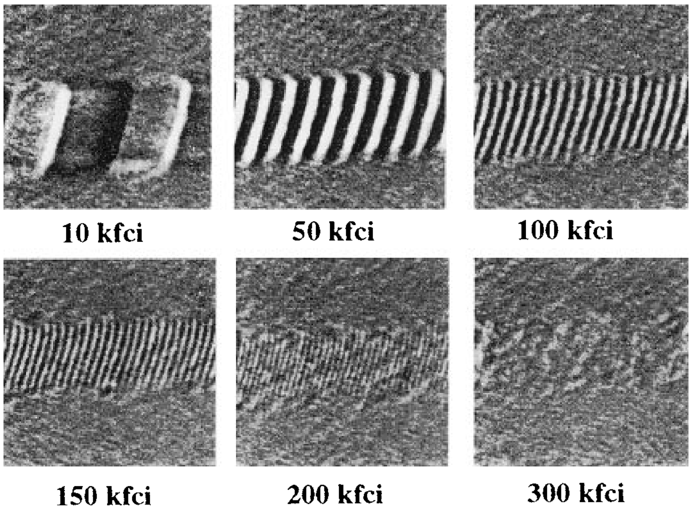

Figure 4. MFM image of data tracks written on a longitudinal hard disk at a range of densities (1 kfci = 390 bits cm^{-1}) (45). Reprinted with permission of the authors and the American Institute of Physics.

Modern implementations of MFM typically interleave a line scan in contact mode (53) for acquisition of the surface topography with a scan where the tip is servoed at a controlled lift height (a few tens of nanometers) above the specimen surface to measure long-range tip–sample interactions (54). The interleaving technique allows for effective separation of topographic information from the magnetic signal. In many MFM designs, detection sensitivity is increased by resonance detection techniques. The tip is excited at the free-resonance frequency of the cantilever and changes of the vibration amplitude, frequency, or phase due to the tip–sample interaction are measured (55,56). Lateral resolution is typically about 40 nm, though resolution as good as 10 nm has been reported (57).

The magnetic interaction between the tip and the specimen is due to a coupling with energy density $-\boldsymbol{H}\cdot\boldsymbol{M}$ where $\boldsymbol{H}$ is the magnetic field above the specimen and $\boldsymbol{M}$ is the tip magnetization. The force on the tip is given by the negative gradient of the energy density integrated over the tip volume. This force causes a deflection of the cantilever or, in the case of resonance detection, leads to a detuning of the free-resonance conditions. The minimum detectable force gradient for a cantilever with spring constant 1 N/m, resonance frequency 100 kHz, vibration amplitude 10 nm, and quality factor 200 is estimated to be better than 10^{-4} N/m (54). If the phase shift is measured, the MFM signal measures the gradient of the force on the tip, which is proportional to the second derivative of the magnetic field above the sample surface, from which the magnetization pattern in the medium must be inferred. The magnetization within the medium cannot be deduced uniquely from the MFM image, so in practice a magnetization pattern is assumed and the calculated field derivatives are compared with the MFM image until agreement is reached (44). It is also possible to image the magnetic field strength directly by using a feedback loop to control an externally applied field (58).

CONCLUSIONS

With bit lengths in hard disk media now below 200 nm, magnetization features of interest in magnetic recording are generally not observable by conventional optical techniques. High-resolution techniques including NFOM, SEM, SEMPA, SPLEEM, EH, Lorentz TEM, and MFM are being pushed to their limits in the competition to provide the most convenient, highest-resolution magnetic images. Instrument design and observation techniques are advancing rapidly, but at the same time, the requirements (higher-resolution images obtained from thinner, lower-moment films having higher coercivity, smaller structural features, and smaller magnetized bits) become more stringent. Thus, imaging needs continue to be at the very limit of our capabilities. SEMPA, SPLEEM, and NFOM instruments continue to be in prototype mode, making comparisons and tool use difficult. Some interesting applications of these techniques have been shown, but for now it appears that LTEM and MFM will continue to be used in most studies of magnetic media. For imaging needs related to magnetic recording heads, such as examination of domain patterns in inductive pole pieces, MOKE is the dominant technique due to its simplicity and applicability to dynamic measurements.

Considering high-density recording media, LTEM continues to offer the highest-resolution two-dimensional map of thin-film magnetization patterns, with resolution in the best cases as good as 10 nm for optimized samples and imaging conditions. However, samples must be carefully selected and are often specially made to allow useful analysis. Imaging can be impeded by grain morphology, substrate topography, substrate material compatibility with sample preparation, and magnetic layer thinness. As the layer thicknesses of real production hard-disk media decrease, the magnetization–thickness product does not provide sufficient electron deflection for the highest-resolution LTEM.

MFM, which measures surface magnetic field independent of film thickness, has become the workhorse of the industry. Its major advantages are that sample preparation is minimal, topographic information is recorded simultaneously, and resolution is good. Approximately 40 nm resolution images are now almost routine on real media, and there is promise of higher resolution with design of sharper probe tips. As a surface technique, MFM resolution is not affected by decreasing magnetic layer thickness, but because MFM measures field gradients above the surface, the results are not necessarily interpretable as bulk magnetic structure. MFM is nondestructive to the media, allowing direct comparisons between micromagnetic properties and recording performance, and the effects of an external applied field can be measured. TEM and MFM continue to have a place in magnetic media research and development. TEM and other electron microscopy techniques will continue to be used in larger research laboratories, while MFM is increasingly important in applications related to analysis of recorded bit patterns.

BIBLIOGRAPHY

1. F. Bitter, On inhomogeneities in the magnetization of ferromagnetic materials, *Phys. Rev.,* **38**: 1903–1905, 1931.
2. F. Bitter, Experiments on the nature of magnetism, *Phys. Rev.,* **41**: 507–515, 1932.
3. K. Goto, M. Ito, and T. Sakurai, Studies on magnetic domains of small particles of barium ferrite by colloid-SEM method, *Jpn. J. Appl. Phys.,* **19**: 1339–1346, 1980.
4. O. Kitakami, T. Sakurai, and Y. Shimada, High density recorded patterns observed by high resolution Bitter scanning electron microscope method, *J. Appl. Phys.,* **79**: 6074–6076, 1996.
5. W. Rave, R. Schafer, and A. Hubert, Quantitative observation of magnetic domains with the magneto-optical Kerr effect, *J. Magn. Magn. Mater.,* **65**: 7–14, 1987.
6. W. W. Clegg et al., Development of a scanning laser microscope for magneto-optic studies of thin magnetic films, *J. Magn. Magn. Mater.,* **95**: 49–57, 1991.
7. E. Betzig et al., Near-field magneto-optics and high density data storage, *Appl. Phys. Lett.,* **61**: 142–144, 1992.
8. T. J. Silva, S. Schultz, and D. Weller, Scanning near-field optical microscope for the imaging of magnetic domains in optically opaque materials, *Appl. Phys. Lett.,* **65**: 658–660, 1994.
9. M. W. J. Prins et al., Near-field magneto-optical imaging in scanning tunneling microscopy, *Appl. Phys. Lett.,* **66**: 1141–1143, 1995.
10. C. Durken, I. V. Shvets, and J. C. Lodder, Observation of magnetic domains using a reflection-mode scanning near-field optical microscope, *Appl. Phys. Lett.,* **70**: 1323–1325, 1997.
11. H. W. Fuller and M. E. Hale, Determination of magnetization distribution in thin films using electron microscopy, *J. Appl. Phys.,* **31**: 238–248, 1960.
12. R. H. Wade, Transmission electron microscope observations of ferromagnetic grain structures, *J. Phys. (Paris) Colloque,* **C2**: 95–109, 1968.
13. J. P. Jakubovics, Lorentz microscopy and applications (TEM and SEM), in U. Valdre and E. Ruedl (eds.), *Electron Microscopy in Materials Science,* Luxembourg: Commission of the European Communities, 1975, Vol. 4, pp. 1303–1403.
14. J. N. Chapman, The investigation of magnetic domain structures in thin foils by electron microscopy, *J. Phys. D.,* **17**: 623–647, 1984.
15. K. Tang et al., Lorentz transmission electron microscopy study of micromagnetic structures in real computer hard disks, *IEEE Trans. Magn.,* **32**: 4130–4132, 1996.
16. J. N. Chapman, M. F. Gillies, and P. P. Freitas, Magnetization reversal process in TbCo-biased spin valves, *J. Appl. Phys.,* **79**: 6452–6454, 1996.
17. B. Y. Wong and D. E. Laughlin, Direct observation of domain walls in NiFe films using high resolution Lorentz microscopy, *J. Appl. Phys.,* **79**: 6455–6457, 1996.
18. S. J. Hefferman, J. N. Chapman, and S. McVitie, In-situ magnetizing experiments on small regularly-shaped permalloy particles, *J. Magn. Magn. Mater.,* **95**: 76–84, 1991.
19. I. Petri et al., Investigations on the stray fields of magnetic read-write heads and their structural reasons, *IEEE Trans. Magn.,* **32**: 4141–4143, 1996.
20. K. Tsuno, Magnetic domain observation by mean of Lorentz electron microscopy with scanning techniques, *Rev. Solid State Sci.,* **2**: 623–658, 1988.
21. J. B. Elsbrock and L. J. Balk, Profiling of micromagnetic stray fields in front of magnetic recording media and heads by means of a SEM, *IEEE Trans. Magn.,* **20**: 866–868, 1984.
22. I. R. McFadyen, Magnetic-domain imaging techniques, *Proc. 51st Annu. Meet. Micr. Soc. Amer.,* **51**: San Francisco, CA: San Francisco Press, 1993, pp. 1022–1023.
23. K. Koike and H. Hayakawa, Observation of magnetic domains with spin-polarized secondary electrons, *J. Appl. Phys.,* **45**: 585–586, 1984.

24. J. Unguris et al., High resolution magnetic microstructure imaging using secondary electron spin polarization analysis in a SEM, *J. Microsc.,* **139**: RP1–2, 1985.
25. J. Unguris et al., Investigations of magnetic microstructures using scanning electron microscopy with spin polarization anlysis, *J. Magn. Magn. Mater.,* **54–57**: 1629–1630, 1986.
26. D. R. Penn, Electron mean-free-path calculations using a model dielectric function, *Phys. Rev. B,* **35**: 482–486, 1987.
27. H. P. Oepen and J. Kirschner, Magnetization distribution of 180° domain walls at Fe(100) single crystal surfaces, *Phys. Rev. Lett.,* **62**: 819–822, 1989.
28. H. Matsuyama and K. Koike, Twenty-nm resolution spin polarized scanning electron microscope, *J. Electron. Microsc.,* **43**: 157–163, 1994.
29. M. R. Scheinfein et al., Scanning electron microscopy with polarization analysis (SEMPA), *Rev. Sci. Instrum.,* **61**: 2501–2506, 1990.
30. H. Pinkvos et al., Spin-polarized low-energy electron microscopy study of the magnetic microstructure of ultra-thin epitaxial cobalt films on W (110), *Ultramicrosc.,* **47**: 339–345, 1992.
31. M. S. Altman et al., Spin polarized low energy electron microscopy of surface magnetic structure, *Mater. Res. Soc. Symp. Proc.,* **232**: 125–132, 1991.
32. D. Gabor, A new microscopic principle, *Nature,* **161**: 777–778, 1948.
33. D. Gabor, Microscopy by reconstructed wave fronts, *Proc. R. Soc. London A,* **197**: 454–487, 1949.
34. A. Tonomura, Applications of electron holography, *Rev. Mod. Phys.,* **59**: 639–669, 1987.
35. J. M. Cowley, Twenty forms of electron holography, *Ultramicrosc.,* **41**: 335–348 1992.
36. A. Tonomura, *Electron Holography,* Berlin: Springer-Verlag, 1993.
37. G. Mollenstedt and H. Duker, Beobachten und Messungen an Biprisma-Interferenzen mit Elektronwellen, *Z. Phys.,* **145**: 377–397, 1956.
38. M. Mankos, M. R. Scheinfein, and J. M. Cowley, Quantitative micromagnetics: electron holography of magnetic thin films and multilayers, *IEEE Trans. Magn.,* **32**: 4150–4155, 1996.
39. D. G. Streblechenko et al., Quantitative magnetometry using electron holography: Field profiles near magnetic force microscope tips, *IEEE Trans. Magn.,* **32**: 4124–4129, 1996.
40. Y. Takahashi et al., Observation of magnetic induction distribution by scanning interference electron microscopy, *Jpn. J. Appl. Phys.,* **33**: L1352–1354, 1994.
41. D. Rugar et al., Magnetic force microscopy: general principles and application to longitudinal recording media, *J. Appl. Phys.,* **68**: 1169–1183, 1990.
42. S. H. Liou et al., High resolution imaging of thin film recording heads by superparamagnetic magnetic force microscopy tips, *Appl. Phys. Lett.,* **70**: 135–137, 1997.
43. R. B. Proksch et al., Magnetic force microscopy of the submicron magnetic assembly in a magnetotactive bacterium, *Appl. Phys. Lett.,* **66**: 2582–2584, 1995.
44. E. D. Dahlberg and J. G. Zhu, Micromagnetic microscopy and modelling, *Phys. Today,* **48** (April): 34–40, 1995.
45. M. E. Schabes et al., Magnetic force microscopy study of track edge effects in longitudinal media, *J. Appl. Phys.,* **81**: 3940–3942, 1997.
46. R. O'Barr et al., Preparation and quantitative magnetic studies of single-domain nickel cylinders, *J. Appl. Phys.,* **79**: 5303–5305, 1996.
47. D. Sarid, *Scanning Force Microscopy,* Oxford: Oxford University Press, 1994.
48. K. Babcock et al., Magnetic force microscopy: recent advances and applications, *Mater. Res. Soc. Symp. Proc.,* **355**: 311–322, 1995.
49. K. Babcock et al., Optimization of thin film tips for magnetic force microscopy, *IEEE Trans. Mag.,* **30**: 4503–4505, 1994.
50. M. Ruehrig et al., Electron beam fabrication and characterization of high resolution magnetic force microscope tips, *J. Appl. Phys.,* **79**: 2913–2919, 1996.
51. G. D. Skidmore and E. D. Dahlberg, Improved spatial resolution in magnetic force microscopy, *Appl. Phys. Lett.,* **71**: 3293–3295, 1997.
52. P. F. Hopkins et al., Superparamagnetic magnetic force microscopy tips, *J. Appl. Phys.,* **79**: 6448–6650, 1996.
53. Q. Zhong et al., Fractured polymer/silica fiber surface studied by tapping mode atomic force microscopy, *Surf. Sci.,* **290**: L688–692, 1993.
54. P. Gruetter, H. J. Mamin, and D. Rugar, Magnetic force microscopy, in R. Wiesendanger and H.-J. Guentherodt (eds.), *Scanning Tunneling Microscopy II,* Springer Series in Surface Sciences, Berlin: Springer-Verlag, 1992, vol. 28, pp. 151–207.
55. Y. Martin, C. C. Williams, and H. K. Wickramasinghe, Atomic force microscope-force mapping and profiling on a sub-100 Å scale, *J. Appl. Phys.,* **61**: 4723–4729, 1987.
56. T. R. Albrecht et al., Frequency modulation detection using high-Q cantilevers for enhanced force microscopy sensitivity, *J. Appl. Phys.,* **69**: 668–673, 1991.
57. P. Gruetter et al., 10-nm resolution by magnetic force microscopy on FeNdB, *J. Appl. Phys.,* **67**: 1437–1441, 1990.
58. R. Proksch et al., Quantitative magnetic field measurements with the magnetic force microscope, *Appl. Phys. Lett.,* **69**: 2599–2601, 1996.

C. A. Ross
Massachusetts Institute of Technology
M. E. Schabes
IBM Almaden Research Center
T. Nolan
Komag Inc.
K. Tang
IBM Research
R. Ranjan
Seagate Magnetics
R. Sinclair
Stanford University